C. R. Chimie 19 (2016) 1642–1655

Contents lists available at ScienceDirect

Comptes Rendus Chimie

www.sciencedirect.com

Full paper/Mémoire

Investigation at the micrometer scale of pancreatic calcifications in chronic pancreatitis by μFTIR spectroscopy and field emission scanning electron microscopy

Jérôme Cros [a, b, *], Dominique Bazin [c, d], Alex Kellum [e], Vinciane Rebours [f, b], Michel Daudon [g, h, i]

[a] AP-HP, Hôpital Beaujon, Department of Pathology, 92000 Clichy, France
[b] INSERM U1149 – Université Paris-7, France
[c] CNRS, LCMCP-UPMC, Collège de France, 11, place Marcellin-Berthelot, 75231 Paris cedex 05, France
[d] LPS, Bât 510, Université Paris-XI, 91405 Orsay, France
[e] Department of Chemistry, Clemson University, Clemson, SC, USA
[f] AP-HP, Hôpital Beaujon, Department of Gastroenterology, 92100 Clichy, France
[g] Sorbonne Universités, UPMC Université Paris-6, UMR S 702, Paris, France
[h] INSERM, UMR S 1155, Paris, France
[i] AP-HP, Hôpital Tenon, Service d'explorations fonctionnelles multidisciplinaires, Paris-6, France

ARTICLE INFO

Article history:
Received 24 February 2015
Accepted 25 June 2015
Available online 22 February 2016

Keywords:
Hereditary pancreatitis
Alcoholic chronic pancreatitis
μFTIR spectroscopy
Field emission scanning electron microscopy

ABSTRACT

A set of pancreatic stones and surgical specimens with chronic pancreatitis from various etiologies has been investigated by μFourier Transform Infra-Red spectroscopy and field emission scanning electron microscopy in order to gather information regarding their chemical composition and their structural characteristics at the mesoscopic scale. These physicochemical data were compared to the medical data of the patients. Regarding the pancreatic stones, the complete set of data underlines the presence of three calcium carbonate polymorphs as well as a great diversity on their spatial distribution (core versus surface), a wide range of protein content and the presence of other phases in a limited number of samples. These results suggest that very different mechanisms are involved in stone formation. The results have been also obtained on pancreas tissues. Chemical diversity also exists for ectopic calcifications. The presence of CA and its amorphous precursor (ACCP) constitutes a real challenge for clinicians, such chemical compounds being associated with biological parameters far from those related to calcium carbonate.

1. Introduction

As underlined by Rosenkranz and Patel [1], stones in biliary and pancreatic ducts constitute pathological calcifications [2–4] that plague hundreds of thousands of patients worldwide every year with symptoms that can be mild (pain) to life threatening (cholangitis, severe acute pancreatitis). This major public health problem has motivated several investigations at the interface between physics, chemistry, and medicine in order to describe at the multiscale the structural and chemical characteristics of such biological entities [4–17]. While obstruction of pancreatic ducts by gallstones is the most common cause for acute pancreatitis, calcium salt deposition within the

* Corresponding author. AP-HP, Hôpital Beaujon, Department of Pathology, 92100 Clichy, France.
E-mail address: jerome.cros@aphp.fr (J. Cros).

http://dx.doi.org/10.1016/j.crci.2015.06.015

pancreas gland is less frequent and results from various pathological conditions. The ultimate aim of the studies is to relate the stone chemistry and structural parameters to pathology in order to better understand the pathogenesis and thus delineate the process of pancreatic stone formation. Such a relationship exists for other pathological calcifications such as kidney stones [18–20] and has been assessed for calcifications present in prostate [21,22], breast [23] and cartilage [24–28].

Several investigations have been performed in order to shed light on the chemistry of pancreatic calculi [4–17]. Their chemical analyses by X-ray scattering have shown that most of them contain calcium carbonate ($CaCO_3$) such as calcite [29], vaterite [30], and aragonite [31]. The presence of these calcium carbonate polymorphs is due to the composition of pancreatic secretion for which the first component is a solution of bicarbonate, Na^+, K^+ and water emitted by the epithelial cells that line the pancreatic ducts. The high level of bicarbonate as well as high values of pH of this alkaline solution explain the presence of calcium carbonates [6]. Other chemical phases such as brushite [7] and Ca phosphate compounds [10] have also been identified. Finally, protein deposits also exist [8,32].

Pancreatic calcifications are mostly seen in advanced stages of chronic pancreatitis. There are many etiologies and some, such as specific forms of hereditary pancreatitis, are associated with an increased risk of pancreatic cancer. Hereditary pancreatitis represents a peculiar form of chronic pancreatitis in which several genes involved in the trypsinogen pathway have been identified [33]. Although they are usually diagnosed earlier than toxic chronic pancreatitis (alcohol related for instance), there is no specific clinical sign and fastidious sequencing of multiple genes is required when the diagnosis is suspected. *PRSS1*, *SPINK1*, and *CFTR* to some extent are the most frequently mutated genes in hereditary pancreatitis [34]. The *PRSS1* gene encodes the cationic trypsinogen that represents 2/3 of the total trypsinogen in the pancreatic juice. Trypsinogen is an inactive precursor of trypsin with capacities of activation and autodigestion. This autodigestion is linked to a particular proteolytic site of the protein in the R122 position. This primary proteolytic site can become resistant in the case of mutations such as the most described R122H [35]. Other reported mutations (>30 described in 2012) can increase the autocatalytic conversion of trypsinogen to active trypsin explaining recurrent acute pancreatitis by intrapancreatic trypsinogen activation. The natural inhibitor of trypsinogen SPINK1 (serine protease inhibitor Kazal type 1) is secreted by the pancreatic acinar cells and can inhibit around 20% of the intrapancreatic trypsin activity. Inactivating mutation may therefore result in trypsin overactivity-related pancreatitis. Several studies demonstrated an association between a SPINK1 mutation (N34S) and chronic pancreatitis, although it is not yet clear how it affects SPINK1 activity ([36] and reviewed in [37]). For CFTR, the mechanism is slightly different. Mutations impairing this transporter function are responsible for a decrease in pancreatic juice bicarbonate concentration resulting in intracanalar protein plugs and calcifications.

In this investigation, pancreas stones and surgical tissue specimens from patients suffering from chronic pancreatitis of various etiologies were investigated in order to assess their physicochemical characteristics and compare them with the clinical data of the patients. Among the different techniques which can obtain significant information on pathological calcifications [38–40], we combined μFTIR spectroscopy [41] and field emission scanning electron microscopy [42] to describe structural characteristics and chemical composition at the micrometer scale. This new class of structural characterization techniques clearly opens a land of opportunities for the understanding of the biochemical parameters that drive the pathogenesis of ectopic calcifications [2–4].

2. Materials and methods

A set of 14 pancreatic stones (Tenon Hospital, Paris, France) without clinical annotation and of 12 surgical specimens of pancreas tissue (Beaujon Hospital, Clichy, France) from patients with chronic pancreatitis were investigated. In the later cohort, the calcifications were microscopic (<5 mm). They were mostly located within small pancreatic ducts or embedded within the pancreatic tissue. There was no common patient between the two cohorts.

Pancreatic stones were analyzed sequentially from the core to the surface by means of selective samples picked up under a stereomicroscope. Then, the samples were mixed with potassium bromide to obtain pellets as previously described in Ref. [43]. The molecular and crystalline composition was determined by infrared spectroscopy using the transmission mode in the wavelength range of 2.5–25 μm (4000–400 cm^{-1}) with a 4 cm^{-1} resolution.

Five micrometer-thick slices of the tissue samples were deposited on low-e microscope slides (MirrIR, Kevley Technologies, Tienta Sciences, Indianapolis). For tissue embedded in paraffin, the paraffin was chemically removed by xylene baths in order to improve the crystal detection under the microscope. Each sample was only named by a study number, without indication of the name of the patient or potential identification data.

A Zeiss SUPRA55-VP SEM was used for the observation of microstructures. This field-emission gun microscope (FE-SEM) operates at 0.5–30 kV. High-resolution observations were obtained by using two secondary electron detectors: an in-lens SE detector and an Everhart–Thornley SE detector. To maintain the integrity of the samples, measurements were taken at low voltage (between 0.5 and 2 kV) without the usual deposits of carbon at the surface of the sample (Fig. 1a). Energy Dispersive X-ray (EDX) spectrometry analyses were also performed. In order to perform Ca cartography, the FE-SEM is operated at 12 kV.

IR microspectroscopy was also performed on an IN10MXmicroscope (Thermo Scientific) for recording large maps. All spectra were collected in ultrafast mode using a 50 μm × 50 μm aperture. The spectra were collected in the 4000–800 cm^{-1} mid-IR range at a resolution of 16 cm^{-1} with one spectrum per pixel. Data analysis of IR spectra and

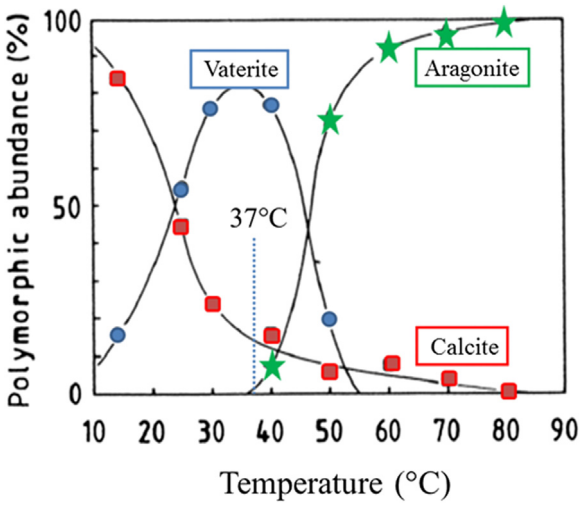

Fig. 1. Abundance of polymorphs as a function of temperature (adapted from Ogino et al. [60]).

chemical images was performed using OMNIC software (Thermo Scientific).

3. Results

In Table 1 the results of stone composition as determined by infrared spectroscopy are summarized. Anhydrous calcium carbonate was the main chemical species in all cases in the form of one or several among the three polymorphs. Calcite was found in all stones while aragonite was identified in 8/14 samples (57.1%) and vaterite in only three calculi (21.4%). Other calcium salts were identified as minor components such as carbapatite in two cases (14.3%) and calcium palmitate in one case (7.1%). The calcium phosphate content was very low (≤5%). By contrast, the protein content was very variable, ranging from about 1% up to 30%. Of note, the highest content of proteins was found in patients presenting with inherited calcifying pancreatitis. In such cases, the stone core was made of proteins while in other pathological conditions it was made of a calcium salt. In one case, the core was predominantly made of calcium palmitate, which suggests a high content of free fatty acids in the pancreatic juice.

In Table 2 the available data regarding pancreatic tissue samples analyzed by infrared microspectroscopy are gathered.

By contrast with pancreatic stones, only two polymorphs of anhydrous calcium carbonate were detected in pancreatic calcifications, i.e., calcite and vaterite. Calcium orthophosphate as apatite was identified in only one case, in association with amorphous carbonated calcium phosphate. Of note, calcium carbonate was not detected in this sample.

4. Discussion

The pancreas acts as an exocrine gland (by producing pancreatic juice which empties into the small intestine via the main pancreatic duct) and an endocrine gland (by producing several hormones including insulin). Pancreatic

Table 1
Chemical composition of pancreatic stones as given by FTIR spectroscopy. Information regarding the associated pathology is also given when available.

Sample	Sex, age (years)	Chemical composition as given by FTIR spectroscopy
242	H	Core and surface: calcite (99%) + traces of CA and proteins
575	F, 26	Core: proteins; surface: calcite ≫ proteins ≫ aragonite average composition: calcite (50%), proteins (30%), and aragonite (20%) pathology: inherited calcifying pancreatitis
5745	F, 71	Core: calcite ≫ aragonite ≫ proteins; surface: aragonite ≫ proteins average composition: aragonite (80%), calcite (15%), and proteins (5%)
8959	H, 43	Core: calcium palmitate ⋙ proteins; surface: calcite ⋙ proteins average composition: calcite (85%), proteins (8%), and calcium palmitate (7%)
9464	H, 55	Core and surface: calcite (99%), proteins (1%)
16232	F, 40	Core: calcite (100%); surface: aragonite ≫ proteins and calcite average composition: aragonite (67%), proteins (13%), calcite (8%), triglycerides (7%), and carbapatite (5%)
16568	H, 62	Core and surface: calcite (90%), proteins (10%)
32274	F, 37	Core: proteins; surface: calcite ≫ proteins, aragonite average composition: calcite (66%), proteins (20%), aragonite (14%) pathology : inherited calcifying pancreatitis
33043	H, 49	Core: calcite ⋙ proteins; surface: calcite ≫ aragonite ≫ proteins average composition: calcite (70%), aragonite (15%), proteins (10%), and vaterite (5%) pathology: alcohol-related chronic pancreatitis
43580	H, 63	Core: calcite ≫ aragonite; surface: calcite ≫ aragonite ≫ proteins ≫ vaterite average composition: calcite (60%), aragonite (20%), proteins (10%), and vaterite (10%)
48440	H, 17	Core: calcite ≫ vaterite; surface: calcite ≫ aragonite, proteins and vaterite average composition: calcite (70%), proteins (15%), aragonite (10%), and vaterite (5%)
59791	H, 41	Core and surface: calcite ≫ proteins average composition: calcite (90%), proteins (10%)
59849	H, 66	Core: calcite ≫ proteins; surface: calcite ≫ aragonite ≫ proteins average composition: calcite (75%), aragonite (15%), and proteins (10%) pathology: alcohol-related chronic pancreatitis
67483	H, 43	Core: calcite ≫ proteins; surface: calcite ≫ vaterite and proteins average composition: calcite (85%), proteins (10%), and vaterite (5%)

Table 2
Physiological and clinical data of the patients and chemical composition of the corresponding tissue samples. (CP: chronic pancreatitis, ACP: alcohol related chronic pancreatitis, IPMN: intraductal papillary and mucinous neoplasm, and ACCP: amorphous carbonated calcium phosphate).

Samples	Age	Disease	Chemical composition of pathological deposits through FTIR spectroscopy
Sample 1 – B0408022_P3_A	36	IPMN w/CP	Glycated proteins
Sample 2 – B0353568_R	36	ACP	Calcite
Sample 3 – B0505143	51	CFTR + SPINK1 CP	Calcite + traces of CA and ACCP
Sample 4 – B0322978	38	Unknown	Vaterite (744 cm^{-1} & 1085 cm^{-1})
Sample 5 – B0448146	31	PRSS1 CP	Vaterite + calcite
Sample 6 – B0515722 (same patient as for sample 3)	52	CFTR + SPINK1 CP	Calcite and trace of CA and ACCP
Sample 7 – B0298452_5C	37	Unknown	Calcite
Sample 8 – B0517376_18	50	PRSS1 CP	Calcite + vaterite
Sample 9 – B0410070_11	49	Unknown	Calcite + vaterite
Sample 10 – 13AG03778_03	48	Cystic fibrosis	ACCP
Sample 11 – 13AG03478 08	71	Unknown	Apatite + ACCP
Sample 12 – 13AG03685_05	52	ACP	Calcite + vaterite

secretion is an alkaline liquid, which contains a variety of enzymes. Pancreatic secretion contains bicarbonate, Na^+, K^+ and water emitted by the epithelial cells that line the pancreatic ducts. Such alkaline solution neutralizes stomach acid so that digestive enzymes work more effectively. This secretion contains also several enzymatic components such as trypsinogen and chymotrypsinogen… In line with its chemical properties (a high level of bicarbonate as well as high values of pH), pancreatic secretion leads to the formation of calcium carbonate.

$CaCO_3$ has a pivotal role in biomineralisation processes in a number of animal species and microorganisms, but it is infrequent in humans with the exception of physiological crystals in the inner ear and pathological calcifications in pancreas and gallbladder. Such biominerals are one of the most common types present in mollusc shells or pearls, eggshells, and corals [44–46] and cyanobacteria [47]. The literature on calcium carbonate is thus quite vast [see for example Refs. 44–56], this system being one of the most widely studied precipitation systems. Most of the studies try to understand their functions which depend on their shape, size, abundance, position versus the biological tissue, and chemical composition. The prominent hallmark of biomineralization is the morphological control during mineral crystallization. In the case of pathological calcifications, the chemical composition as well as the crystal morphology are also two key parameters to establish a significant link with the disease [18,57–63] and has motivated this investigation by SEM and μFTIR spectroscopy.

Different species of calcium carbonate exist. Starting with the most stable one, we have the anhydrous species ($CaCO_3$) namely calcite, aragonite, and vaterite, the hydrated species such as monohydrocalcite ($CaCO_3 \cdot H_2O$) or Ikaite ($CaCO_3 \cdot 6H_2O$) and finally the amorphous one $CaCO_3$ which may contain water molecules [64,65]. Note that Levi-Kalisman et al. [66] have underlined that several kinds of amorphous carbonate exist, their stability depending on the presence of other compounds such as phosphates. Moreover, J. Ihli et al. [67] showed that amorphous calcium carbonate can dehydrate before crystallizing, both in solution and in air. One of the striking points of this investigation is related to the fact that the loss of the final water fraction – comprising less than 15% of the total – triggers crystallization. Finally, in the case of pathological calcifications, it can be interesting to consider the publication of Ogino et al. [68], which have assessed the abundance of polymorphs as a function of temperature as illustrated in Fig. 1.

The space group of the most stable species, i.e. calcite, is *R*3*c* with $a = 6361$ Å and $\alpha = 46°6'$ [69–71]. In fact, in the crystal nucleation stage, calcite is the most stable form while aragonite becomes more stable when the crystal is large enough for the bulk lattice energy to outweigh the surface energy terms [72]. Calcite crystals display rhombohedra with a square, a morphology in line with their crystallographic structure [73]. Other possibilities (twin crystals) have been considered. Morphologies of calcite crystals can be controlled by impurities [74] such as Mg [75] or peptides [76]. In the case of aragonite, the space group is Pmcn with $a = 4.94$ Å, $b = 7.94$ Å and $c = 5.72$ Å, while for the vaterite the system is hexagonal ($a = 4.12$ Å, $c = 8.556$ Å) [29,37]. In fact, using aberration-corrected high-resolution transmission electron microscopy, L. Kabalah-Amitai et al. [30] found that vaterite is actually composed of at least two different crystallographic structures that coexist within a pseudo-single crystal. Regarding amorphous calcium carbonate, Breýeviû and Nielsen [77] isolated ACC by freeze drying and found the powder consisting of spherical particles with diameters in the order of 50–400 nm. Note that complex calcium carbonate entities can be obtained. For example, S.S. Wang et al. [78] have obtained calcium carbonate microspheres with calcite equatorial loops and vaterite spherical cores.

4.1. Pancreatic stones

At the macroscopic scale, pancreatic stones are associated with different morphologies. In Fig. 2, three pancreatic stones are visualized. While the first one (Fig. 2a) is constituted to an agglomeration of rod shaped entities resembling corals, the two other stones (Fig. 2b,c) have a round shape and exhibit a calcite cockle with a core of protein.

A set of SEM micrographs of pancreatic stones at the micrometer scale shows very different structures. In Fig. 3a,b, sharp acicular entities are visible in contrast to very smooth entities that seem to be embedded in an organic film (Fig. 3c–e) or in contact with tissue or cells

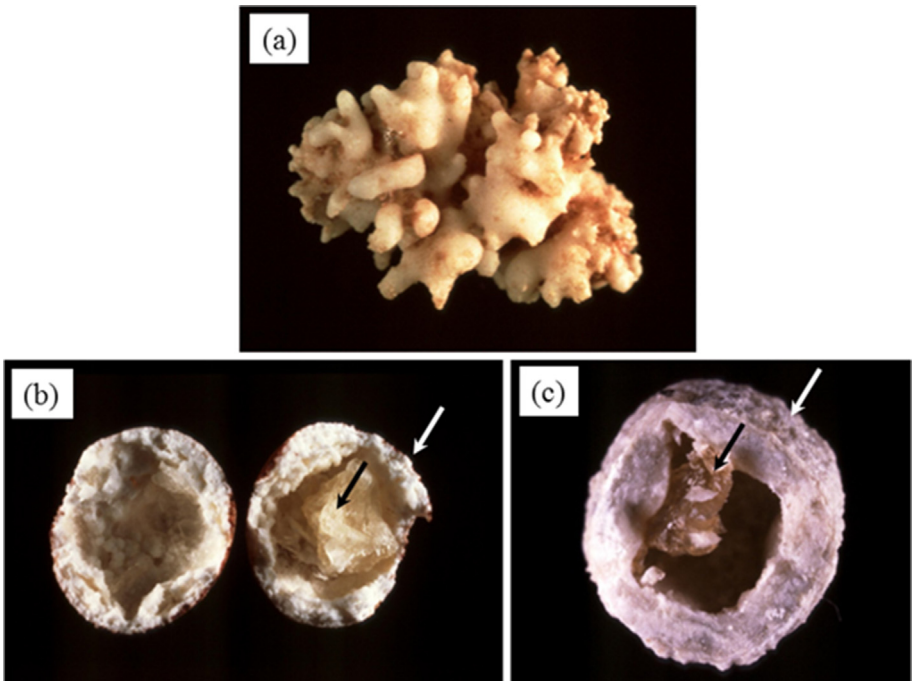

Fig. 2. Pancreatic calculi. At the macroscopic scale, different morphologies exist (agglomeration of rod shaped entities (a) or round shape with a calcite cockle and a protein core (b and c).

(Fig. 3f). Such organic part may be constituted by lithostathine, a protein that was initially considered as an inhibitor of calcium carbonate crystal growth in pancreas ducts where the supersaturation is common for that chemical species [79–82]. However, more recent studies suggest that lithostathine could act as a non-specific inhibitor similarly to other proteins such as albumin [83]. In patients suffering from familial calcifying pancreatitis, mutations of the gene involved in lithostathine synthesis are responsible for tissue calcification either because of a quantitative defect in lithostathine production or, as observed in Fig. 2b,c, by production of partly or entirely inactive mutated proteins that are able to precipitate in the pancreas, serving as a template for further calcium carbonate deposition. Such a mechanism may thus favor the formation of pancreatic stones that may obstruct the main duct and induce acute and/or chronic pancreatitis. Of note, an analog of lithostathine was also identified in the kidney tissue, where, by an adsorption process on the crystal surface, it could protect against the potential heterogeneous nucleation of weddellite on calcite crystals [84]. Finally, observations of crystallites with smooth surfaces have been already done in the case of cystine kidney stones in patients treated by alkali or/and thiol therapy [85].

SEM observations offer an opportunity to describe the complex biochemical parameters which drive the growing mechanisms of pancreatic stones. H. Harada et al. [6] have noticed that crystalline calcite showed spiral and epitaxial growth along with findings of dissolution, resembling cholesterol crystals of gallstones. These authors supposed that pancreatic stones were probably formed through central core formation and layered growth of a shell. A.C. Schultz et al. [11] underline that a central amorphous material was observed in 30% of the pancreatic stones indicating that the protein present at the core of the pancreatic stones constitutes a nucleus for pancreatic stones, an hypothesis already proposed by H. Sarles et al. [5] in patients with alcoholic pancreatitis.

Regarding a possible link between pancreatic stones and diseases, pancreatic calcifications have long been considered specific for chronic pancreatitis [86,87]. In a recent study, A. Campisi et al. [88] have shown that pancreatic calcifications are observed in a wide spectrum of pancreatic diseases. These authors underline the fact that certain findings (parenchymal calcifications, diffuse distribution, intraductal calcifications, parenchymal atrophy, and cystic lesions) are noted more often in chronic pancreatitis than in other pancreatic diseases harboring calcifications. Unfortunately, this investigation was based only on cardinal computed tomography and it was thus quite difficult to discuss the chemical composition of the pancreatic calcifications.

In our study, FTIR spectroscopy points out the presence of these calcium carbonate polymorphs as well as a great diversity on the spatial distribution of these three calcium carbonates in the core and at the surface of the pancreatic stones. Due to the low number of samples, it is quite difficult to extract a link with disease from these structural data. However, our results suggest that different mechanisms are involved in stone formation. For example, in inherited calcifying pancreatitis, the protein content of the stones was especially high and the core, by contrast to other pathological conditions, was mainly composed of protein agglomerates. In another case, the

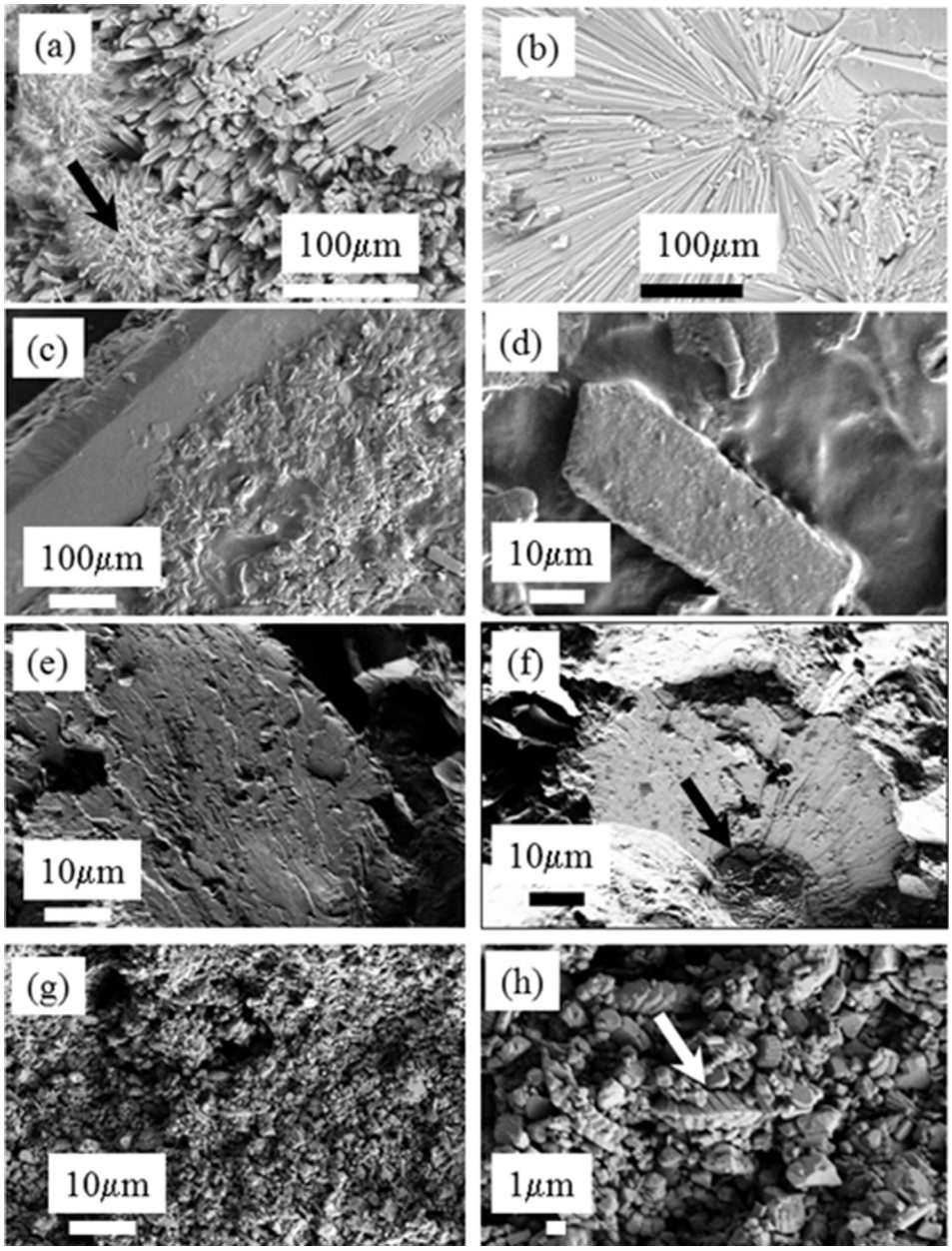

Fig. 3. Different morphologies observed in pancreatic stones. (a) and (b) Large acicular entities with well-defined edges and faces; (c), (d), and (e) structures with smooth edges and numerous surface defaults, some have a circular shape probably due to the presence of tissues or cells; (f), (g), and (h) well-defined structures observed in tiny calcite crystals at the micrometer scale.

core of the stone was made of a fatty acid, crystallized as calcium salt, which appears to be a very uncommon condition. Unfortunately, we have no clinical data for this patient.

4.2. Surgical specimens with chronic pancreatitis

Regarding μFTIR spectroscopy, since the pioneering work of T.B. Morse [89], mid-Infrared absorption bands of

Table 3
Infrared frequencies of calcite, aragonite and vaterite according to C.E. Weir and E.R. Lippincott [91].

	ν_1	ν_2	ν_3	ν_4
Calcite	1087 cm^{-1} (weak)	881 cm^{-1}	1432 cm^{-1}	712 cm^{-1}
Aragonite	1087 cm^{-1}	866 cm^{-1}	1430 & 1550 cm^{-1}	703 & 715 cm^{-1}
Vaterite	1090 cm^{-1}	850 & 878 cm^{-1}	1450 cm^{-1}	711 & 747 cm^{-1}

calcium carbonate have been extensively studied [90–97]. From a fundamental point of view, isolated planar ion XO_3 displaying a trigonal symmetry has four fundamental modes of vibration, the symmetric stretching, ν_1, the out of plane bending, ν_2, the doubly degenerate antisymmetric stretching, ν_3, and the doubly degenerate planar bending, ν_4. In a crystalline solid containing more than 1 molecule per unit cell, symmetry considerations indicate that all

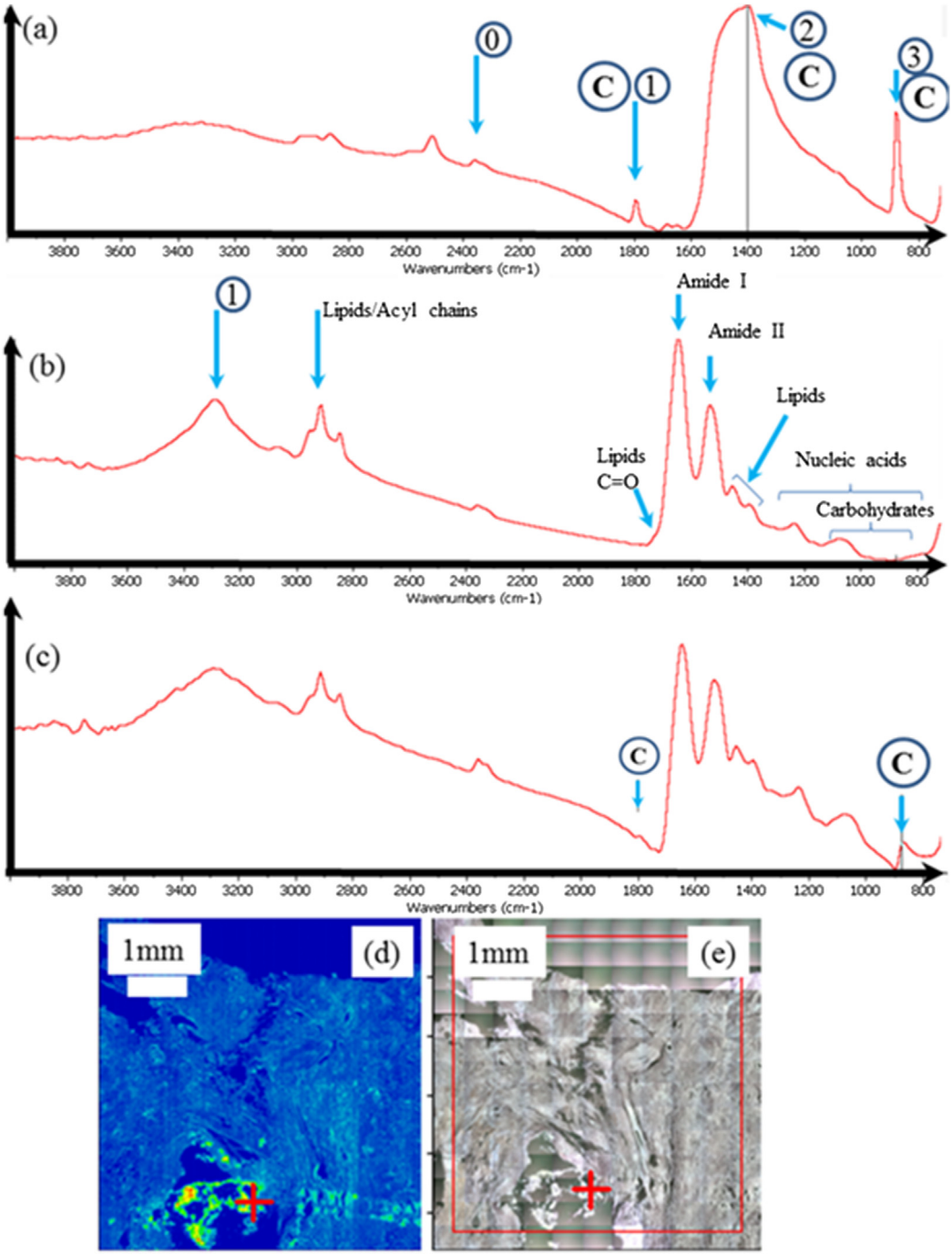

Fig. 4. Sample 5: (a) typical IR absorption bands of the calcite calcification; 0 corresponds to the residual absorption of CO_2 present in the room experiments while 1,2, and 3 are related respectively to the combination band, ν_3 and ν_2 IR absorption bands of calcite; (b) IR absorption bands of a biological tissue where the different contributions coming from have been indicated; (c) generally the IR spectrum contains contributions coming from both calcifications (here made of calcite) and tissues; (d) classical analysis of FTIR data is to compare the spatial distribution of a chemical compound selected by an IR absorption band and (e) the optical photography. Of note, the red cross in (d) and (e) indicates where the IR spectrum has been collected.

modes may be active. Following the investigations by C.E. Weir and E.R. Lippincott [91], these four fundamental modes are represented in Table 3 for the different polymorphs of $CaCO_3$.

These calculated values are close to the ones measured for the different compounds. These characteristic bands of calcite are observed at 712 cm^{-1} (ν_4; in-plane bending) and 875 cm^{-1} (ν_2: O–C–O out-of-plane bending) while the ν_1 symmetric stretching band at 1086 cm^{-1} is inactive in the IR mode (active in the Raman mode) [41,98,99]. For aragonite (resp. vaterite), absorption bands are, respectively, 699 and 713, 854, and 1082 cm^{-1} (resp. 713 and 744, 876, and 1086 cm^{-1}) [41,91,95]. As underlined by N.V. Vagenas et al. [96], the positions of the wavenumbers are unique for each carbonate mineral and are thus diagnostic of their mineralogy. Note that the combination band near 1800 cm^{-1} (1799 cm^{-1} for calcite and 1788 cm^{-1} for aragonite) is composed of contributions from combination of the ν_3 asymmetric stretching and the ν_6 and ν_8 external modes of the carbonate groups and Ca^{2+} ions [100–102].

In Fig. 4, typical FTIR spectra corresponding to the calcification (4a), to the tissue (4b) or to a mixing of calcification and tissue (4c) are presented. Here, the calcification is made of calcite and we can identify quite easily its three IR absorption bands (1799–1390–875 cm^{-1}) versus vaterite (1403–1085–744 cm^{-1}).

In Fig. 4b, the IR spectrum shows the presence of the major molecular species, amide I and II from the protein constituents of the pancreatic tissue [103–107]. The amide functional group combines the features of amines and ketones because it has both the N–H and the C=O bonds. In ketones, carbonyl compounds (those that contain the C=O functional group) are in the middle of the carbon chain while in aldehydes, this group is at the end. The most characteristic band in amines appears as a weak to medium IR broad band in the range of about 3200–3600 cm^{-1} and is due to the N–H bond stretching. More precisely, two N–H stretching peaks may be observed, one near 3350 cm^{-1} and one near 3180 cm^{-1}, from asymmetric and symmetric vibrations, respectively.

In biological tissues, the bands at 1640 cm^{-1} and 1546 cm^{-1} correspond to amide I C=O stretching mode and amide II N–H bending and C–N stretching in proteins. As underlined by L.M Miller and P. Dumas [108], the vibrational frequency of the amide I (C=O) band can be significantly affected by different hydrogen-bonding environments for α-helix, β-sheet, turn, and unordered structures. In this case, it is possible to deconvolute the absorption bands in different contributions. Other data analysis processes are possible [109–112]. Correlation factors can be calculated in order to perform the correlation analysis. Finally, principal component analysis can also be used to extract relevant information from the spectral dataset.

In Fig. 4c, both contributions coming from the tissue and the calcification are visible. It is the case when the size of the calcification is less than the size of the beam (here a few microns). Finally, from the FTIR data it is possible to obtain quite simply the spatial distribution of the different

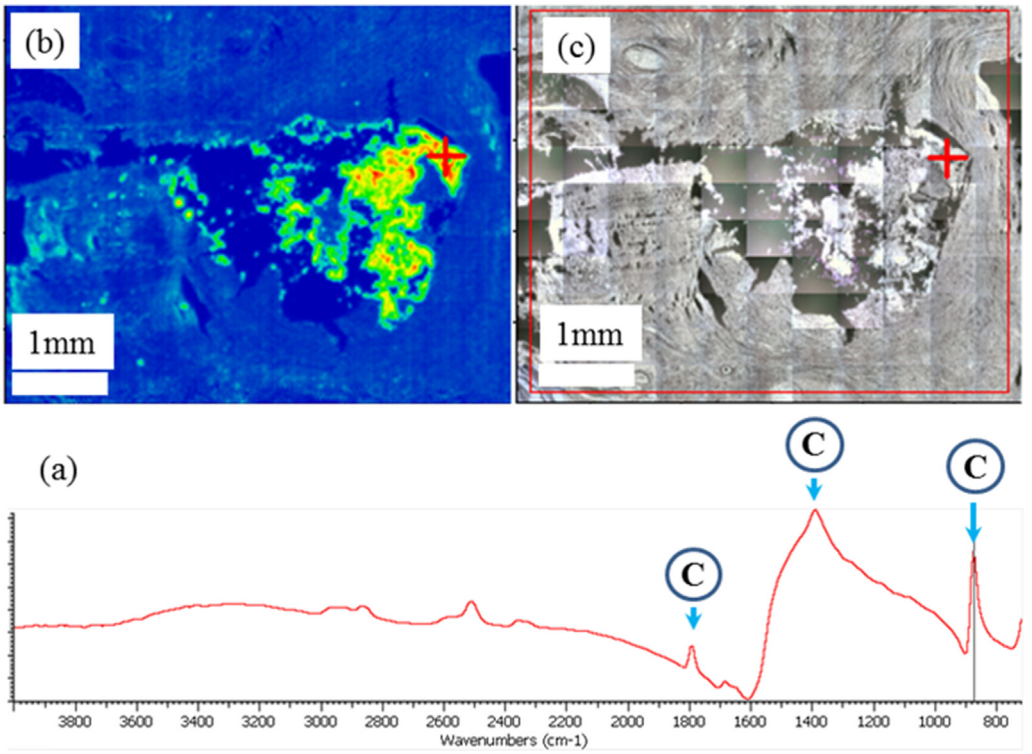

Fig. 5. Sample 8: (a) typical IR absorption bands of the calcite calcification recorded at the level of the red cross in Fig. 5c; (b) Spatial repartition of the calcite ectopic calcification as measured through the intensity of the IR absorption band at 875 cm^{-1}; (c) Optical map at the same scale.

molecular species that have been identified through their IR absorption bands. In order to obtain the spatial distribution of calcite (Fig. 4d), its absorption band has been selected (in that part of the IR spectra, only contribution coming from calcite is present). For the clinician, it is possible to localize precisely the calcification in the tissue through a comparison with the optical map (Fig. 4e).

Even in the case of large calcifications (Fig. 5), it is possible to perform such analysis. For sample 8, information regarding the localization of large calcifications (larger than 1 mm) can be obtained.

For sample 9, which corresponds to an unidentified etiology, two calcium carbonate polymorphs have been identified. Thanks to the high sensitivity of FTIR

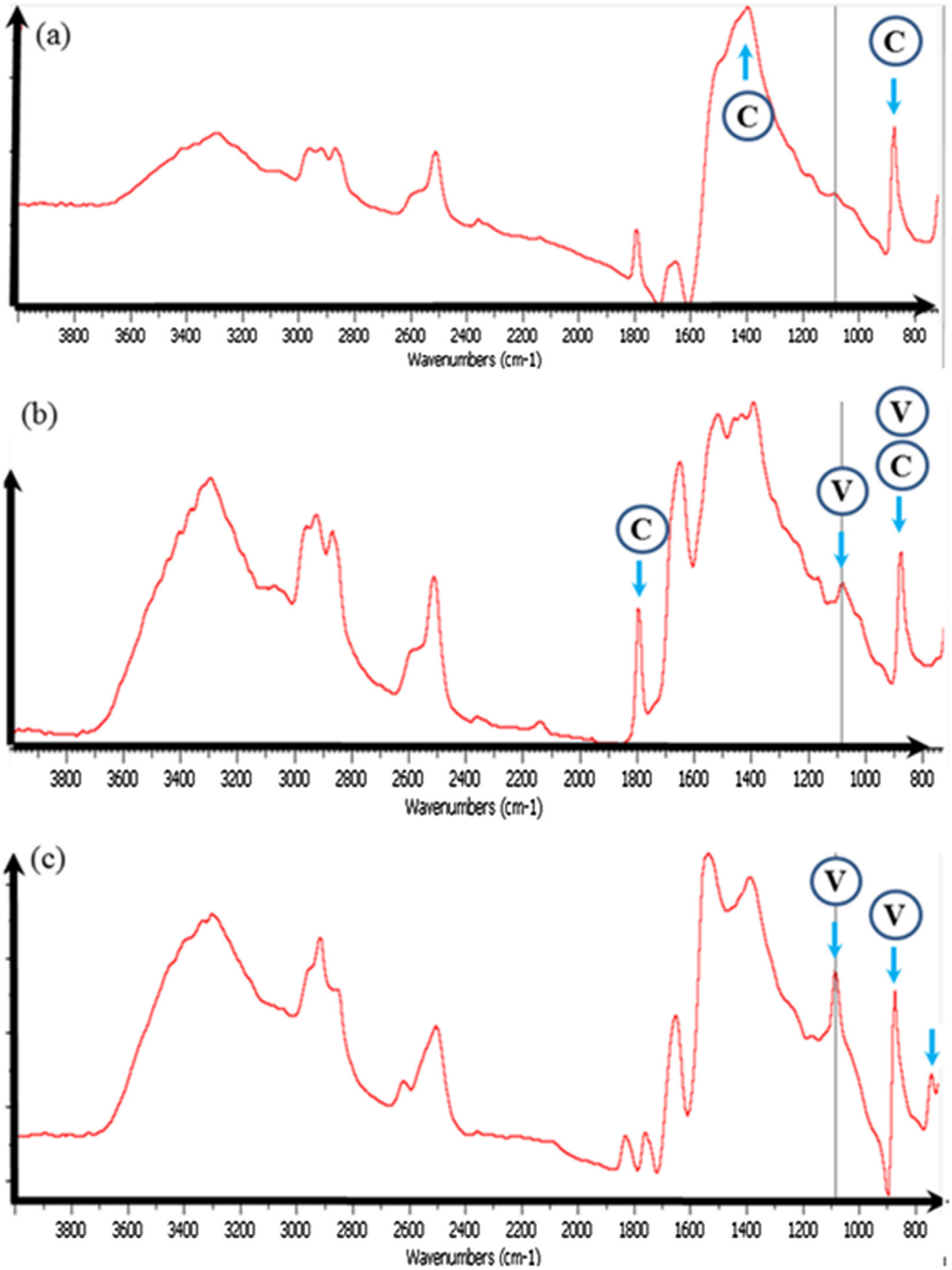

Fig. 6. Sample 9: (a) typical IR absorption bands of the calcite calcification; (b) the presence of small proportions of vaterite induced the observation of a supplementary peak at 1085 cm^{-1}; (c) typical IR absorption bands of a calcification made of vaterite.

spectroscopy, it is possible to distinguish between calcite (Fig. 6a) and vaterite (Fig. 6c). When the two polymorphs are present, the IR spectrum is simply a combination of the two IR spectra (Fig. 6b).

For sample 10, which corresponds to a patient with cystic fibrosis, a precise observation of the IR absorption spectra underlines (arrows) the possible presence of different chemical phases in addition to proteins such as silicate (contamination?) (Fig. 7a), mucopolysaccharides, without (Fig. 7b) and with small amounts of calcium phosphate (Fig. 7c), or Ca phosphate apatite alone (Fig. 7d).

It is also possible to gather information regarding the morphology of the ectopic calcification after its chemical identification through FTIR spectroscopy. For sample 3 coming from a patient with chronic pancreatitis (Fig. 8), FE-SEM observations have been performed after the acquisition of a FTIR map on the very same sample. In that case, details at the micrometer scale can be obtained. As we can see, the faces of calcite crystallites are not well defined suggesting that we have at the micrometer scale a mixing between mineral and proteins.

Finally, in another sample of pancreatic tissue, FTIR experiments underlined the presence of ectopic calcifications made of Ca phosphate apatite. A careful examination of the IR absorption at 1030 cm^{-1} indicates the presence of Ca phosphate apatite and amorphous Ca phosphate apatite. Also, this Ca phosphate apatite is carbonated as indicated by the presence of carbonate IR absorption bands (Fig. 9).

Etiologies of chronic calcifying pancreatitis are numerous and may sometimes be combined. A robust tool to help define the etiology would be greatly appreciated,

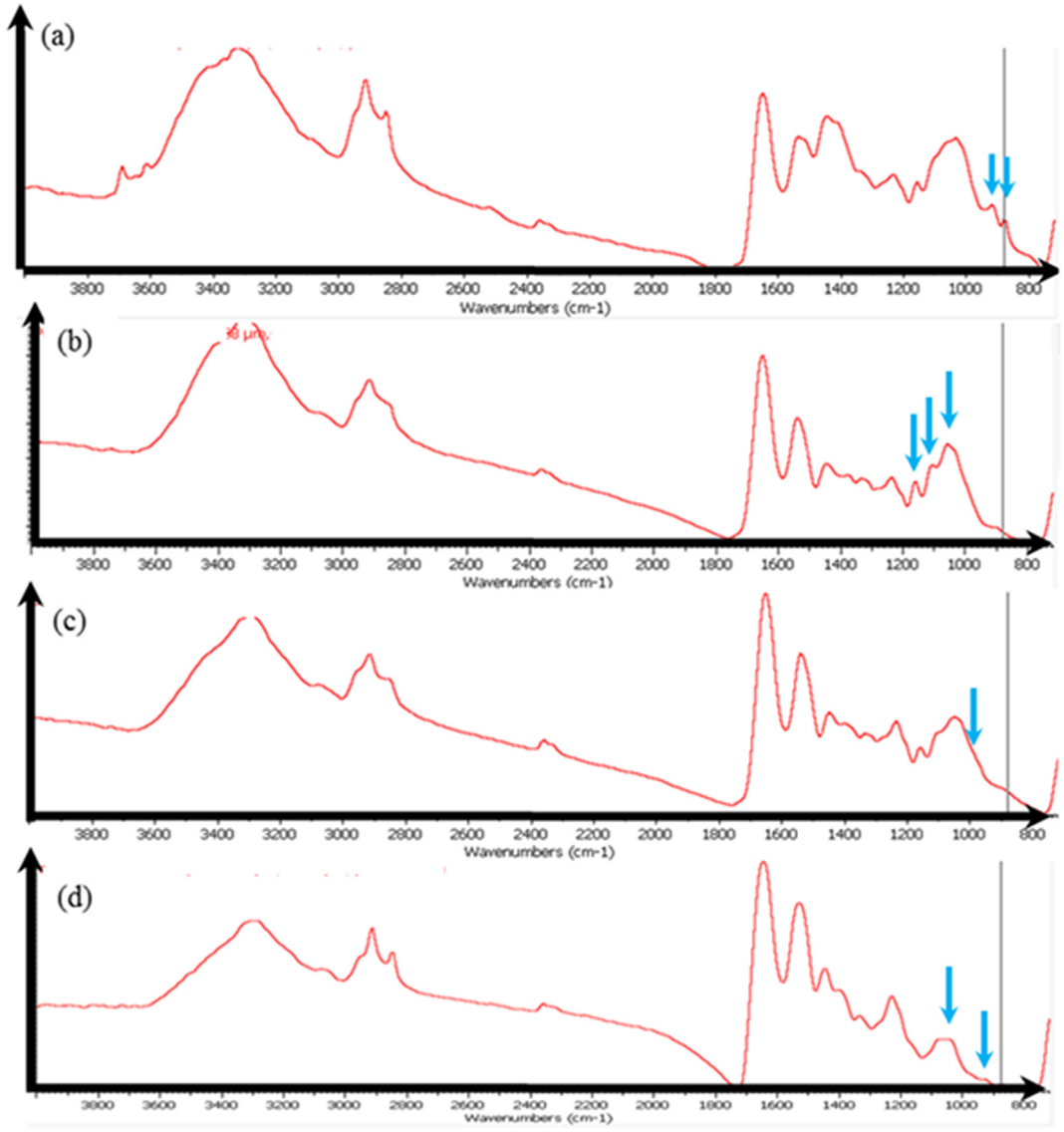

Fig. 7. Sample 10: the IR spectrum seems to show, in addition to proteins, the presence of silicate (a), of mucopolysaccharides (b), of mucopolysaccharides and calcium phosphate (low content) (c), and of Ca phosphate apatite (d).

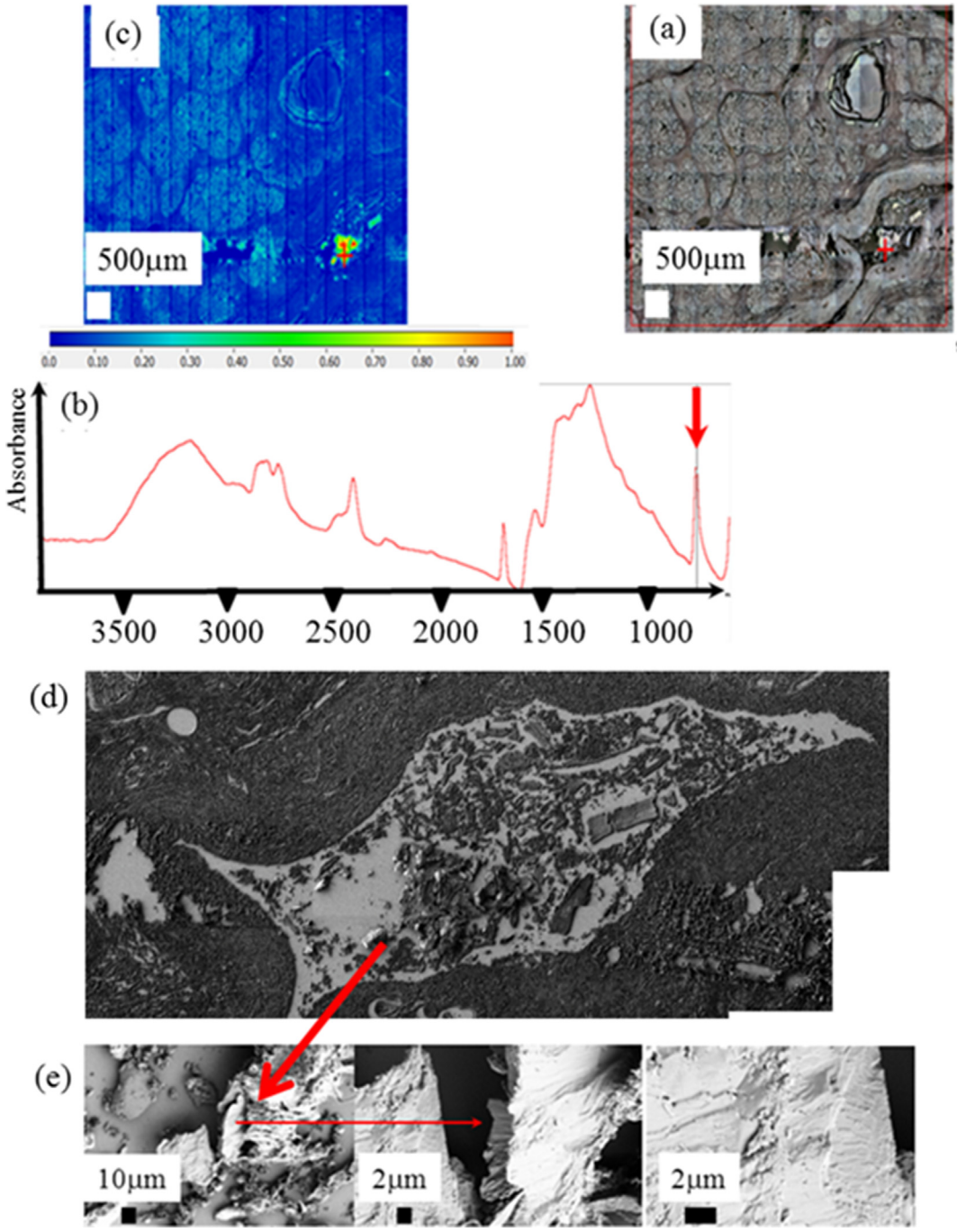

Fig. 8. Set of data collected for sample 3: (a) optical microscope observation; (b) typical infra red spectrum; (c) spatial distribution of calcite corresponding to the spatial distribution of the intensity of the IR absorption bands at 875 cm^{-1}; (d) topology of the very sample is obtained through SEM; (e) details of the sample surface visualized at higher magnification.

especially in cases of hereditary pancreatitis in which multiple gene sequencing is long and expensive. Chronic pancreatitis is often managed medically. Surgical specimens are rare resulting in a very small number of patients for a given etiology. It did not seem that one type of calcification composition was restricted to one etiology but larger groups are necessary to definitively conclude. Close relationships have been observed between pancreatic calcifications and the metabolism of calcium. It was reported that chronic pancreatitis is a possible cause of hypocalcemia. By contrast, hypercalcemic states of primary hyperparathyroidism may induce pancreatic calcifications [113–114]. Calcium phosphate deposits were found in human pancreatic adenocarcinoma (Capan-1) cell cultures

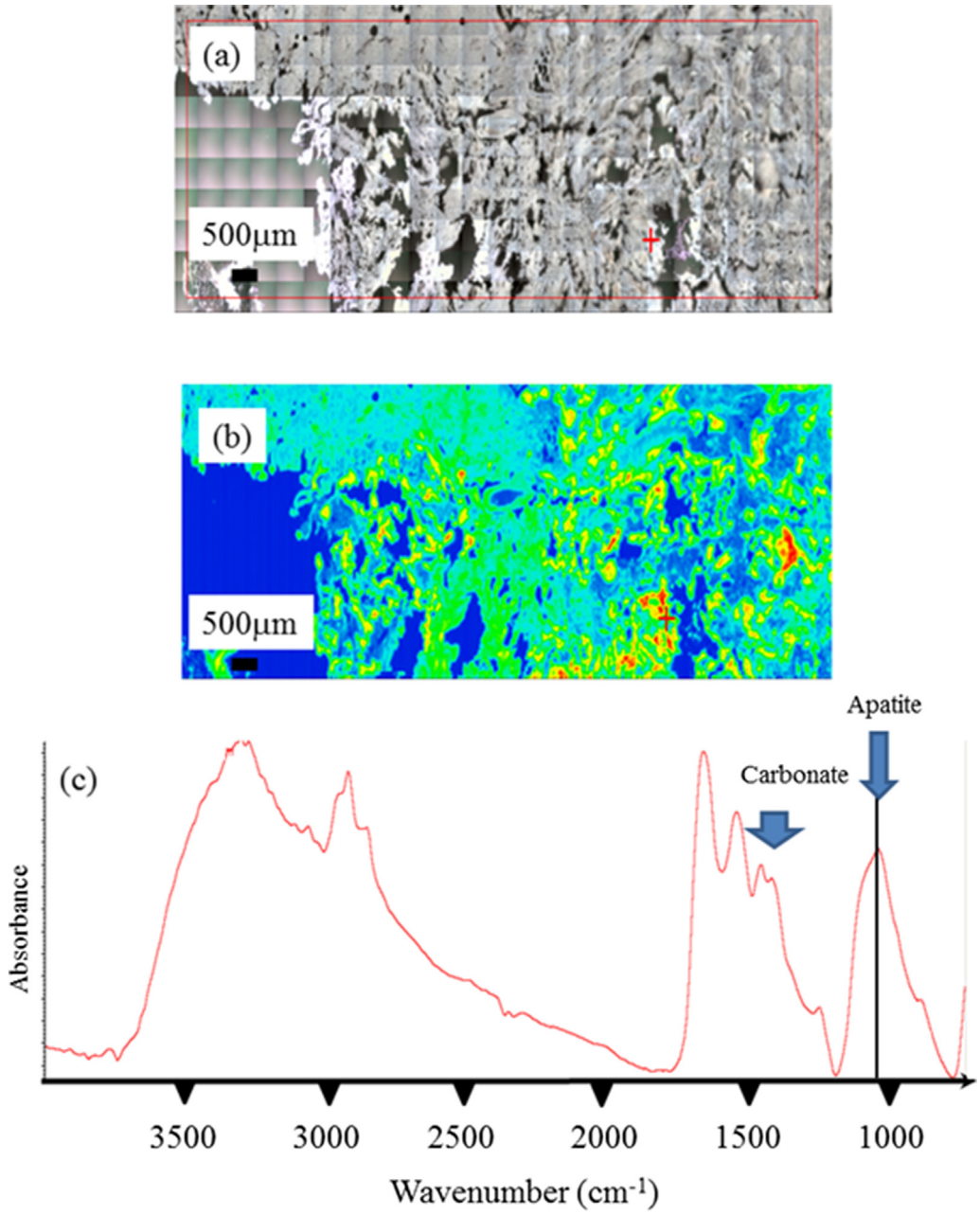

Fig. 9. Sample 11. (a) Optical microscope observations; (b) spatial distribution of the apatite in the sample; (c) IR absorption spectrum pointing out the presence of microcalcifications made of highly carbonated apatite. Note the presence of ACCP through the attenuated shoulder (around 1100 cm^{-1}) of the ν_3 absorption band of apatite at 1030 cm^{-1}.

[115]. Low citrate concentration, high calcium diffusion from interstitium to pancreatic juice, local protein precipitation and other alterations in the pancreatic juice composition are possible factors involved in pancreatic calcifications [109]. We can expect differences in the chemical form, crystalline phases, accurate distribution and abundance of calcifications according to the etiology. Our results suggest that further investigations should be performed to relate more precisely pancreatic calcifications and the etiology of pancreatitis, as demonstrated for other tissues such as kidney [18–20].

5. Conclusion

Even if stones in biliary and pancreatic ducts constitute a major public health problem, the number of investigations based on physical techniques remains quite limited. Our investigation clearly shows that only

techniques such as last generation FTIR and FE-SEM experimental devices offer a chemical and structural description at the mesoscopic scale and are able to bring to clinicians a significant description of pathological calcifications [2–4].

Regarding the pancreatic stones, FTIR spectroscopy and FE-SEM observations underline the presence of the three calcium carbonate polymorphs as well as a great diversity on their spatial distribution (core versus surface). These results suggest that very different mechanisms are involved in stone formation. For example, in inherited calcifying pancreatitis, the protein content of the stones was especially high and the core, by contrast to other pathological conditions, was mainly composed of protein agglomerates. In another case, the core of the stone was made of a fatty acid, crystallized as calcium salt, which appears to be a very uncommon condition.

Major results have been also obtained on pancreas tissues. Chemical diversity exists also for ectopic calcifications. The presence of CA and its amorphous precursor (ACCP) constitutes a real challenge for clinicians, such chemical compounds being associated with biological parameters far from those related to calcium carbonate.

Due to the limited number of samples in this investigation, it was not possible to establish a possible relationship between the calcifications' composition and the chronic pancreatitis etiology. These pathologies are rare and the small number of subjects may have masked relevant associations. However, the chemical diversity of calcium deposits (carbonate or phosphate) suggests a variety of pathological conditions involved in pancreatic calcifications. The precise crystalline form of calcium carbonate or calcium phosphate identified in the tissue could be simply a marker of the timing of the calcification process regardless of the causing mechanism. Studies are in progress to better understand the actual relationships between crystals and pathology as performed in other tissues.

Acknowledgments

This work was supported by the Physics and Chemistry Institutes of CNRS and by contracts ANR-09-BLAN-0120-02, ANR-12-BS08-0022, ANR-13-JSV-10010-01, convergence UPMC CVG1205 and CORDDIM-2013-COD130042.

References

[1] L. Rosenkranz, S.N. Patel, Gastrointest. Endosc. Clin. N. Am. 22 (2012) 435.
[2] D. Bazin, M. Daudon, C. Combes, C. Rey, Chem. Rev. 112 (2012) 5092.
[3] D. Bazin, M. Daudon, J. Phys. D Appl. Phys. 45 (2012) 383001.
[4] D. Bazin, J.-P. Haymann, E. Letavernier, J. Rode, M. Daudon, Presse Med. 43 (2014) 135.
[5] H. Sarles, Gastroenterology 66 (1974) 604.
[6] H. Harada, M. Takeda, J. Tanaka, H. Miki, K. Ochi, I. Kimura, Gastroenterol. Jpn. 18 (1983) 530.
[7] A.L. Rodgers, Micron. Microsc. Acta 14 (1983) 219.
[8] E.W. Moore, H.J. Vérine, J. Lab Clin. Med. 106 (1985) 611.
[9] A.L. Rodgers, M. Spector, Calcif Tissue Int. 39 (1986) 342.
[10] A. Noda, T. Takayama, Y. Ogawa, Y. Sugimoto, T. Shibata, Y. Horiguchi, S. Kameya, Y. Nakanishi, Gastroenterol. Jpn. 21 (1986) 255.
[11] A.C. Schultz, P.B. Moore, P.J. Geevarhese, C.S. Pitchumoni, Dig. Dis. Sci. 31 (1986) 476.
[12] C.S. Pitchumoni, K.V. Viswanathan, P.J. Gee Varghese, P.A. Banks, Pancreas 2 (1987) 152.
[13] Z.P. Jing, Zhonghua Wai Ke Za Zhi 28 (1990) 421.
[14] H. Tohda, Y. Tsuchiya, T. Kobayashi, H. Kishiro, T. Yanagisawa, J. Electron. Microsc. (Tokyo) 43 (1994) 57.
[15] L. de Pablo-Galan, M.D. Lastra-Azpilicueta, Rev. Mex. Cienc. Geol. 14 (1997) 78.
[16] K.V. Narasimhulu, N.O. Gopal, J.L. Rao, N. Vijayalakshmi, S. Natarajan, R. Surendran, V. Mohan, Biophys. Chem. 114 (2005) 137.
[17] E.K. Choi, G.A. Lehman, Korean J. Intern. Med. 27 (2012) 20.
[18] M. Daudon, C.A. Bader, P. Jungers, Scan. Microsc. 7 (1993) 1081.
[19] M. Daudon, R.J. Reveillaud, Néphrologie 5 (1984) 195.
[20] M. Daudon, L'Eurobiologiste XXVII 203 (1993) 35.
[21] A. Dessombz, P. Méria, D. Bazin, E. Foy, S. Rouzière, R. Weil, M. Daudon, Prog. Urol. 21 (2011) 940.
[22] A. Dessombz, P. Méria, D. Bazin, M. Daudon, PLoS One 7 (2012) e51691.
[23] T.C. Holme, M.M. Reis, A. Thompson, A. Robertson, D. Parham, P. Hickman, P.E. Preece, Eur. Surg. Oncol. 19 (1993) 250.
[24] H.-K. Ea, C. Nguyen, D. Bazin, A. Bianchi, J. Guicheux, P. Reboul, M. Daudon, F. Lioté, Arthritis Rheum. 63 (2011) 10.
[25] C. Nguyen, H.-K. Ea, D. Bazin, M. Daudon, F. Lioté, Arthritis Rheum. 62 (2010) 2829.
[26] C. Nguyen, H.K. Ea, D. Thiaudière, S. Reguer, D. Hannouche, M. Daudon, F. Lioté, D. Bazin, J. Synchrotron Radiat. 18 (2011) 475.
[27] C. Nguyen, D. Bazin, M. Daudon, A. Chatron-Colliet, D. Hannouche, A. Bianchi, D. Côme, A. So, N. Busso, F. Lioté, H.-K. Ea, Arthritis Res. Ther. 15 (2013) R103.
[28] H.-K. Ea, V. Chobaz, C. Nguyen, S. Nasi, P. van Lent, M. Daudon, A. Dessombz, D. Bazin, G. McCarthy, B. Jolles-Haeberli, A. Ives, D. Van Linthoudt, A. So, F. Lioté, N. Busso, PLoS One 8 (2013) e57352.
[29] A.J. Skinner, J.P. Lafemina, H.J.F. Jansen, Am. Mineral. 79 (1994) 205.
[30] L. Kabalah-Amitai, B. Mayzel, Y. Kauffmann, A.N. Fitch, L. Bloch, P.U.P.A. Gilbert, B. Pokroy, Science 340 (2013) 454.
[31] J.P.R. De Villiers, Am. Mineral. 56 (1971) 758.
[32] L. Multigner, M. Daudon, G. Montalto, A. de Caro, J.-P. Étienne, H. Sarles, N. Engl. J. Med. 314 (1986) 248.
[33] N. Teich, J. Mössner, Best Pract. Res. Clin. Gastroenterol. 22 (2008) 115.
[34] M.H. Derikx, J.P. Drenth, Best Pract. Res. Clin. Gastroenterol. 24 (2010) 251.
[35] R. Pfützer, E. Myers, S. Applebaum-Shapiro, R. Finch, I. Ellis, J. Neoptolemos, J.A. Kant, D.C. Whitcomb, Gut 50 (2002) 271.
[36] R.H. Pfützer, M.M. Barmada, A.P. Brunskill, R. Finch, P.S. Hart, J. Neoptolemos, W.F. Furey, D.C. Whitcomb, Gastroenterology 119 (2000) 615.
[37] J.M. Chen, C. Férec, Annu. Rev. Genomics Hum. Genet. 10 (2009) 63.
[38] D. Bazin, M. Daudon, P. Chevallier, S. Rouzière, E. Elkaim, D. Thiaudière, B. Fayard, E. Foy, P.A. Albouy, G. André, G. Matzen, E. Véron, Ann. Biol. Clin. 64 (2006) 125.
[39] M. Daudon, D. Bazin, J. Phys. Conf. Ser. 425 (2013) 022006.
[40] D. Bazin, M. Daudon, Ann. Biol. Clin., (in press).
[41] N. Quy-Dao, M. Daudon, Infrared and Raman Spectra of Calculi, Elsevier, 1997.
[42] F. Brisset, M. Repoux (Eds.), Microscopie électronique à balayage et microanalyse, EDP Sciences, 2008.
[43] M. Daudon, M.F. Protat, R.J. Reveillaud, Ann. Biol. Clin. 36 (1978) 475.
[44] H.A. Lowenstam, S. Weiner, On Biomineralization, Oxford University Press, 1989.
[45] R. Lakes, Nature 361 (1993) 511.
[46] J. Xiao, Y. Zhu, J. Juan, Q. Ruan, Y. Zheng, L. Cheng, L. Wang, F. Xu, Mod. Phys. Lett. B 23 (2009) 3695.
[47] K. Benzerara, F. Skouri-Panet, J. Li, C. Férard, M. Gugger, T. Laurent, E. Couradeau, M. Ragon, J. Cosmidis, N. Menguy, I. Margaret-Oliver, R. Tavera, P. López-García, D. Moreira, Proc. Natl. Acad. Sci. USA 111 (2014) 10933.
[48] K. Benzerara, T.H. Yoon, T. Tyliszczak, B. Constantz, A.M. Spormann, G.E. Brown Jr., Geobiology 2 (2004) 249.
[49] K. Benzerara, N. Menguy, P. Lopez-Garcia, T.-H. Yoon, J. Kazmierczak, T. Tyliszczak, F. Guyot, G.E. Brown Jr., PNAS 103 (2006) 9440.
[50] K.B. Lee, S.B. Park, Y.N. Jang, S.W.J. Lee, J. Colloid Interface Sci. 355 (2011) 54.
[51] O. Cizer, C. Rodriguez-Navarro, E. Ruiz-Agudo, J. Elsen, D. Van Gemert, K. Van Balen, J. Mat. Sci. 47 (2012) 6151.

[52] K. Lee, W. Wagermaier, A. Masic, K.P. Kommareddy, M. Bennet, I. Manjubala, S.-W. Lee, S.B. Park, H. Cölfen, P. Fratzl, Nat. Commun. 3 (2012) 725.
[53] J.H.E. Cartwright, A.G. Checa, J.D. Gale, D. Gebauer, C.I. Sainz-Díaz, Angew. Chem. Int. Ed. 51 (2012) 11960.
[54] J. De Yoreo, Nat. Mater. 12 (2013) 284.
[55] B. Fritz, A. Clément, G. Montes-Hernandez, C. Noguera, Cryst. Eng. Comm. 15 (2013) 3392.
[56] L.B. Gower, Chem. Rev. 108 (2008) 4551.
[57] M. Daudon, O. Traxer, P. Jungers, D. Bazin, AIP Conf. Proc. 900 (2007) 26.
[58] M. Daudon, P. Jungers, D. Bazin, New Eng. J. Med. 359 (2008) 100.
[59] M. Daudon, P. Jungers, D. Bazin, AIP Conf. Proc. 1049 (2008) 199.
[60] M. Daudon, D. Bazin, G. André, P. Jungers, A. Cousson, P. Chevallier, E. Véron, G. Matzen, J. Appl. Crystallogr. 42 (2009) 109.
[61] X. Carpentier, M. Daudon, O. Traxer, P. Jungers, A. Mazouyes, G. Matzen, E. Véron, D. Bazin, Urology 73 (2009) 968.
[62] D. Bazin, G. André, R. Weil, G. Matzen, E. Veron, X. Carpentier, M. Daudon, Urology 79 (2012) 786.
[63] A. Dessombz, E. Letavernier, J.-P. Haymann, D. Bazin, M. Daudon., J. Urol., (in press).
[64] T. Yong-Jin Han, J. Aizenberg, Chem. Mater. 20 (2008) 1064.
[65] Y. Politi, R.A. Metzler, M. Abrecht, B. Gilbert, F.H. Wilt, I. Sagi, L. Addadi, S. Weiner, P.U.P.A. Gilbert, PNAS 105 (2008) 17362.
[66] Y. Levi-Kalisman, S. Raz, S. Weiner, L. Addadi, I. Sagi, Adv. Funct. Mat. 12 (2002) 43.
[67] J. Ihli, W.C. Wong, E.H. Noel, Y.-Y. Kim, A.N. Kulak, H.K. Christenson, M.J. Duer, F.C. Meldrum, Nat. Commun. 5 (2014) 3169.
[68] T. Ogino, T. Suzuki, K. Sawada, Geochim. Cosmochim. Acta 51 (1987) 2757.
[69] G. Behrens, L.T. Kuhn, R. Ubic, A.H. Heuer, Spectrosc. Lett. 28 (1995) 983.
[70] J. Dedek, Le Carbonate de Chaux, Librairie Universitaire Louvain, 1966.
[71] H. Teghidet, Etude de la cristallisation contrôlée de la calcite par voie électrochimique. Effet desions étrangers au système calco-carbonique sur la nucléation-croissance de la calcite, UPMC, 2012.
[72] N.H. de Leeuw, S.C. Parker, J. Phys. Chem. B 102 (1998) 2914.
[73] M. Van Meerssche, J. Feneau-Dupont, Introduction à la Cristallographie et àla Chimie Structurale, Vander, Louvain, Cesson, 1973.
[74] M. Ukrainczyk, J. Kontrec, D. Kralj, J. Colloid Interface Sci. 329 (2009) 89.
[75] E. Loste, R.M. Wilson, R. Seshadric, F.C. Meldrum, J. Cryst. Growth 254 (2003) 206.
[76] D.B. DeOliveira, R.A. Laursen, J. Am. Chem. Soc. 119 (1997) 10627.
[77] L. Breýeviû, A.E. Nielsen, J. Cryst. Growth 98 (1989) 504.
[78] S.S. Wang, A. Picker, H. Cölfen, A.-W. Xu, Angew. Chem. Int. Ed. 52 (2013) 6317.
[79] H. Sarles, Ann. Gastroenterol. Hepatol. 22 (1986) 37.
[80] A.M. De Caro, J.-J. Bonicel, P. Rouimi, D. De Caro, H. Sarles, M. Rovery, Eur. J. Biochem. 168 (1987) 201.
[81] D. Giorgi, J.-P. Bernard, S. Rouquier, J. Iovanna, H. Sarles, J.C. Dagorn, Clin. Invest. 84 (1989) 100.
[82] M. Provensal-Cheylan, A. Mariani, J.-P. Bemard, H. Sarles, P. Dupuy, Pancreas 4 (1989) 680.
[83] L. Patard, J.Y. Lallemand, V. Stoven, J.O.P. 4 (2003) 92.
[84] J.M. Verdier, B. Dussol, P. Casanova, M. Daudon, P. Dupuy, P. Berthezene, R. Boistelle, Y. Berland, J.C. Dagorn, Eur. J. Clin. Invest. 22 (1992) 469.
[85] D. Bazin, M. Daudon, G. André, R. Weil, E. Véron, G. Matzen, J. Appl. Crystallogr. 47 (2014) 719.
[86] M.L. Steer, I. Waxman, S. Freedman, N. Engl. J. Med. 332 (1995) 1482.
[87] E.V. Loftus Jr., B.A. Olivares-Pakzad, K.P. Batts, M.C. Adkins, D.H. Stephens, M.G. Sarr, E.P. DiMagno, Gastroenterology 110 (1996) 1909.
[88] A. Campisi, G. Brancatelli, M.-P. Vullierme, P. Levy, P. Ruzniewski, V. Vilgrain, Clin. Radiol. 64 (2009) 903.
[89] T.B. Morse, AstroPhys. J. 26 (1907) 225.
[90] H.H. Adler, P.F. Kerr, Am. Mineral. 47 (1962) 700.
[91] C.E. Weir, E.R. Lippincott, J. Res. NBS A 65A (1961) 173.
[92] G. Hertzberg, Molecular Spectra and Molecular Structure, in: Infrared and Raman Spectra of Polyatomic Molecules, seventh ed., vol. II, D. Van Nostrand Co., New York, N.Y., 1956, p. 178.
[93] D.F. Hornig, J. Chem. Phys. 16 (1948) 1063.
[94] R.S. Halford, J. Chem. Phys. 14 (1946) 8.
[95] S. Gunasekaran, G. Anbalagan, S. Pandi, J. Raman Spectrosc. 37 (2006) 892.
[96] N.V. Vagenas, A. Gatsouli, C.G. Kontoyannis, Talanta 59 (2003) 831.
[97] D. Lou, F. Sun, L. Li, Chin. Opt. Lett. 05 (2007) 370.
[98] J.A. Gadsden (Ed.), Infrared Spectra of Minerals and Related Inorganic Compounds, Butterworths, New York, 1975.
[99] D.R. Taylor, R.S. Crowther, J.C. Cozart, P. Sharrock, J. Wu, R.D. Soloway, Hepatology 22 (1995) 488.
[100] C. Wang, J. Zhao, X. Zhao, H. Bala, Z. Wang, Powder Technol. 163 (2006), 134.9090.
[101] K.H. Hellwege, W. Lesch, M. Plihal, G. Schaack, Z. Phys. 232 (1970) 61.
[102] P. Gillet, P. Mcmillan, J. Schott, J. Badro, A. Grzechnik, Geochim. Cosmochim. Acta 60 (1996) 3471.
[103] G. Müller, W. Wäsche, U. Bindig, K. Liebold, Laser Phys. 9 (1999) 348.
[104] Y.-J. Chen, Y.-D. Cheng, H.-Y. Liu, P.-Y. Lin, C.-S. Wang, Chang Gung Med. J. 29 (2006) 518.
[105] Z. Movasaghi, S. Rehman, I. Ur Rehman, Appl. Spectrosc. Rev. 43 (2008) 134.
[106] F. Le Naour, M.-P. Bralet, D. Debois, C. Sandt, C. Guettier, P. Dumas, A. Brunelle, O. Laprévote, PLoS One 4 (2009) e7408.
[107] P. Bassan, A. Sachdeva, A. Kohler, C. Hughes, A. Henderson, J. Boyle, J.H. Shanks, M. Brown, N.W. Clarke, P. Gardner, Analyst 137 (2012) 1370.
[108] L.M. Miller, P. Dumas, Curr. Opin. Struct. Biol. 20 (2010) 649.
[109] J. Kong, S. Yu, Acta Biochim. Biophys. Sin. 39 (2007) 549.
[110] A. Grunenwald, C. Keyser, A.M. Sautereau, E. Crubézy, B. Ludes, C. Drouet, J. Archaeol. Sci. 49 (2014) 134.
[111] J.R. Schoonover, R. Marx, W.R. Nichols, Vib. Spectrosc. 35 (2004) 239.
[112] M. De Luca, W. Terouzi, G. Ioele, F. Kzaiber, A. Oussama, F. Oliverio, R. Tauler, G. Ragno, Food Chem. 124 (2011) 1113.
[113] P. Layer, H. Goebell, Schweiz Med. Wochenschr. 119 (1989) 1655.
[114] B. Carnaille, C. Oudar, F. Pattou, F. Combemale, J. Rocha, C. Proye, Aust. N. Z. J. Surg. 68 (2) (1998 Feb) 117–119.
[115] E. Hollande, J.-H. Levrat di Donato, M. Fanjul, C. Palevody, M. Daumas, J. Puech, G. Ratovo, Biol. Cell. 69 (1990) 191.